A Detailed Global Model for Modeling and Optical Diagnostics of Low Power Propulsion Devices Fed by CO_2

IEPC-2019-682

Presented at the 36th International Electric Propulsion Conference
University of Vienna • Vienna, Austria
September 15-20, 2019

Chloe Berenguer[1] and Konstantinos Katsonis[2]
DEDALOS Ltd., Thessaloniki, 54645, Greece

Georg Herdrich[3] and Hendrik Burghaus[4]
Institute of Space Systems (IRS), Stuttgart, Germany

Abstract: A Detailed Global Model developed by DEDALOS Ltd for CO_2 plasma study in space and laboratory is used here for electric thruster characterization and optical emission spectroscopy diagnostics based on the obtained plasma components composition diagrams, on the functioning diagrams and on the concomitant theoretical first and second oxygen and carbon spectra. Comparison of our theoretical results including theoretical spectra with experimental ones obtained in IRS, is addressed in particular, taking into consideration that the experimental spectra do not come from a thruster but from a IPG run with CO_2 for Mars entry investigation.

Nomenclature

ξ_{TOT} = total ionization percentage
ABET = Air Breathing Electric Thruster
CO2DGM = CO_2 Detailed Global Model
DEDALOS = Data Evaluation and Diagnostics ALgorithms Of Systems Ltd
DGM = Detailed Global Model
ET = Electric Thruster
FD = Functioning Diagram
GM = Global Model
HelT = Helicon type Thruster
HMO = High Mars Orbit
IPG = Inductively heated Plasma Generator
IRS = Institut für RaumfahrtSysteme, university of Stuttgart
ISRU = *in situ* Resource Utilization
L = cylinder lenght
LMO = Low Mars Orbit
MATM = Mars ATMosphere
n_e = electron density

1 Project Manager, berenguer.dedalos@gmail.com.
2 Director, katsonis.dedalos@gmail.com.
3 Head, Plasma Wind Tunnels and Electric Space Propulsion, herdrich@irs.uni-stuttgart.de.
4 PhD student, hburghaus@irs.uni-stuttgart.de.

NMT = Near Mars Trips
OES = Optical Emission Spectroscopy
p = pressure
P_{ABS} = absorbed power
PCC = Plasma Components Composition
Q_{TOT} = total flow rate
R = cylinder radius
T_e = electron temperature
ThSpec = theoretical spectra
VLMO = Very Low Mars Orbit

1. Introduction

A Detailed Global Model for CO_2 plasma study in space[1,2] and laboratory[3,4], CO2DGM, which has been developed by *DEDALOS Ltd* has been extended in order to provide theoretical spectra (ThSpec) also of carbon species, besides the oxygen ones. This double calculation of ThSpecs aims to improve plasma diagnostics application by non-perturbing Optical Emission Spectroscopy (OES) to CO_2-fueled prototype electric thrusters (ET) meant for Mars based missions with *in situ* Resource Utilisation (ISRU) propellant from the Mars ATMosphere (MATM) which is composed essentially (about 90 %) by CO_2 gas[5] and also to studies of entry in the Mars atmosphere addressed previously (see Ref. 6 and references therein). CO2DGM resulted notably to theoretical characterization and to non-perturbing Optical Emission Spectroscopy (OES) diagnostics of on ground prototype thrusters based in the obtained Plasma Components Composition (PCC) diagrams, of the Functioning Diagrams (FD) and of the concomitant theoretical mainly first and second oxygen and carbon spectra[7]. It allows for preview, characterization, diagnostics and monitoring of CO_2-fueled ETs[3,4]. These tasks are obtained using the following main CO2DGM outputs :

PCC diagrams, allowing for the evaluation of the electron density and temperature and the densities of the various ET plasma components. For a given form factor, these are depending mainly on the plasma pressure, on the absorbed electric power and on the feed of the selected CO_2 propellant.

FD diagrams, providing the ionization percentage of each of the plasma components following iso-baric and iso-thermal curves. For a given form factor and a selected feed, the total ionization level depends on the total pressure and on the absorbed power. Thus, we can obtain a thrust preview and optimize the ET functioning.

ThSpecs, calculated in various ET functioning conditions. Absolute intensity values of the spectral lines composing each ThSpec in comparison with the experimental ones, obtainable by acquisition of the plasma emission spectra, allow for OES, a powerful non perturbing diagnostics method which avoids all of the drawbacks of the frequently used handy Langmuir probes. Detailed study of the ThSpec is a prerequisite to obtain satisfactory OES results, required for ET characterization and monitoring.

Here we first address ET technology by conveniently adapting the CO2DGM parameters to those prevailing specifically in a rather low power class prototype fed by CO_2 . However, CO2DGM is adaptable to a large absorbed energy region and to various ET form factors and types allowing for their preview, characterization, diagnostics and monitoring. As we discussed lately[4], when using MATM as ET propellant the additional nitrogen and argon play only a secondary role. Therefore, in the present contribution we address characterization of prototype ETs fed by MATM on the basis of a modeling addressing solely CO_2 as propellant. The proposed ISRU technology allows for important payload increase and a considerable extension of the ET functioning, the next limit being imposed by the erosion of the plasma facing surface parts. The serious problem of fuel transport from Earth (or even from the Earth atmosphere or from the Moon) is then satisfactorily resolved, at least in what concerns the fuel generating the thrust needed to raise and keep satellites in Low and Very Low Mars Orbits (LMO, VLMO) and for local trips in the Mars region including its satellites Phobos and Demos. With the s/c payload and lifetime greatly increased by ISRU technology for missions based on MATM, we are facing a situation totally analogous to the one of Air Breathing Electric Thruster (ABET) technology, while using MATM as propellant instead of the Earth atmospheric remnants[8,9]. Such a disruptive technology mission constitutes an innovation to be developed only after tools as CO2DGM which are necessary for the feasibility demonstration and for the optimization of the CO_2-fueled ETs are made available.

A preview of the main species amount present in CO_2-fueled prototypes, namely carbon, oxygen and CO including their ions and also of the electron density n_e and temperature T_e values, is obtained and discussed by using PCC diagrams for selected values of absorbed power, CO_2 propellant feed and pressure. Analysis of the corresponding functioning regimes is performed and illustrated on the basis of a dedicated FD. Concomitant ThSpecs calculations have been also carried out. Further to oxygen ThSpecs which were calculated for developing propulsion plasma OES diagnostics, the possibility to calculate also carbon spectra has been added in the present CO2DGM version, thus facilitating the ET characterization by comparing the oxygen theoretical

spectra to the carbon ones.

Although CO2DGM was developed aiming ET technology, it can support modeling and diagnostics of CO_2 plasma in general. On this direction we compare our theoretical results including ThSpecs calculated in various conditions with the experimental ones obtained in *IRS,* taking into consideration that the experimental spectra do not refer to an ET but were acquired from a IPG fed with CO_2 aiming investigation of Mars entry.

After this introduction, the composition and the properties of the plasma created from CO_2 in various conditions are investigated. This concerns low power class CO_2-fueled ET prototypes with Total Flow Rate (Q_{TOT}) of 20 sccm, which are addressed in Section 2. Results belonging to total flow rates of Q_{TOT} = 50 sccm are reviewed in Section 3, for somewhat higher P_{ABS} values to sustain ionization. Finally, entry in CO_2 atmospheres under various conditions is addressed on the basis of CO2DGM results in Section 4. In Section 5, the corresponding calculated CO_2 spectra of interest to atmospheric entry are compared with experimental ones provided by *IRS*, leading to an illustration of OES diagnostics. Finally, conclusions on this work are contained in Section 6.

2. PCC and FD diagrams addressing the main plasma components of electric thrusters

In this section, CO2DGM parameters are conveniently adapted to those prevailing in CO_2-fueled ET prototypes with the Mars atmosphere in mind. Preview of the main species densities in a prototype, namely CO_2, CO, oxygen and carbon, including their ions and molecules, is obtained by CO2DGM together with the electron density n_e and temperature T_e values. PCC diagrams address adequate values of the CO_2 propellant feed Q_{TOT}, absorbed power P_{ABS} and pressure p for the adequate form factor. The corresponding functioning regimes are investigated, analyzed and illustrated on the basis of FDs. In order to obtain detailed results and to provide a thorough support for OES diagnostics, extended sets of data concerning the neutral and the singly, doubly and trebly ionized oxygen and carbon species have been specifically included in the fundamental equations of the model. These consist of a *power balance equation* plus the *statistical equations* of the main plasma species[10]. Thus, CO2DGM is able to describe the effects of the present atomic and ionic structures in a realistic manner, leading also to detailed calculation of the theoretical spectral lines belonging to the ET plasma. Data pertaining to the molecules of interest are also included in the model. CO2DGM evaluates the P_{ABS} losses belonging to the thruster functioning conditions. Thus, it results to realistic mean values of the thruster plasma parameters, as was reported elsewhere[11,12]. A comparison of CO_2-fueled ETs functioning with results obtained by feeding by other propellants, either of ISRU technology or other commonly addressed propellants as Xe or I, has been made available lately[13]. Results including specifically plasma formed in CO_2 atmosphere entry has been also addressed[14].

When focusing on low pressure CO_2 plasma properties of interest to ISRU type VLMO / LMO /HMO electric thrusters fed by the MATM components, the influence of the nitrogen presence in the Mars atmosphere on the functioning of MATM breathing ETs is neglected, in view of previous studies results[3].

The P_{ABS} values concerning PCC presented in this section are 60 W and 180 W. Evidently, P_{ABS} of interest depends on the feed technology selected (direct CO_2 breathing or collection in an adequate propellant vessel), on the thruster type and form factor and on the amount of the used propellant. While PCC diagrams illustrate the constitution of the propellant inside the ET as calculated by the model, synoptic FDs contribute to analyze the thruster functioning. We remind that FDs give the ionization percentage as a function of the pressure by two sets of curves, with each of them pertaining to a defined value of P_{ABS} or of T_e. Note that an alternate form of FD diagrams is also possible, describing the thruster functioning dependence on P_{ABS} , with the parametric curves referring to values of T_e and p.

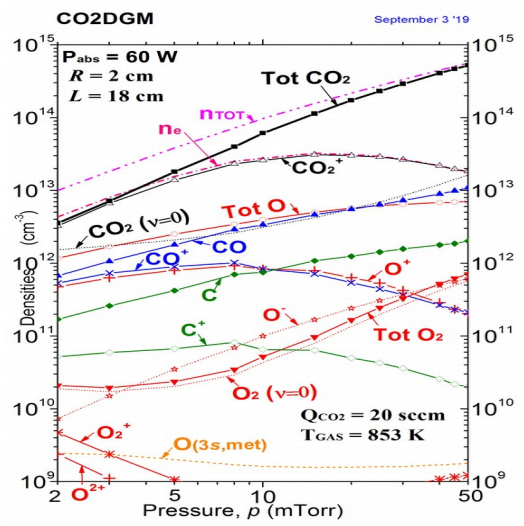

Fig. 1. Pressure depending PCC for 60 W absorbed power

From the numerous analyses of CO2DGM results pertaining to different P_{abs} values we present here two cases with pressure values spanning the region from 2 mTorr to 50 mTorr, in order to obtain a preview of the expected abundances of the various plasma components. The two cases analyzed and compared in this section present pressure depending log – log PCC diagrams spanning the 10^9 cm^{-3} to 10^{15} cm^{-3} region and concern P_{abs} values of 60 W for Fig. 1 and of 180 W for Fig. 2. They pertain both to a form factor of L = 18 cm length and of R = 2 cm radius, with typical CO_2

feed of Q_{TOT} = 20 sccm.

A simple inspection of CO2DGM results for P_{abs}= 60 W illustrated in Fig. 1 shows that the total CO_2 density is higher than this of any other constituent and approach the total density n_{TOT} when pressure increases. This indicates a low CO_2 dissociation. CO_2^+ is the next abundant constituent, but after about 20 mTorr diminishes, still remaining very abundant. This means that CO_2 is strongly ionized while all the other ions present much lower importance as the difference between electron and CO_2^+ presence is very small. Total O and CO densities remain comparable and increase steadily with pressure approaching the CO_2^+ values. C abundance is quite low but follows steadily the O one. CO^+ and O^+ ions have similar values for all pressures and C^+ ions are one order of magnitude less present but they all vary in a similar way, loosing their importance for high pressures. Thus, although presence of O_2 starts with very low values at 2 mTorr, after about 10 mTorr increases fast with pressure and exceeds the CO^+ and O^+ ones. Abundance of O^- species starts from low values, but with increasing pressure arrives to the level of O_2 . Finally, the presence of O_2^+ and of O^{2+} is negligible and diminishing when pressure increases, while this of the metastable O (3*s*) species, very small, remains steady.

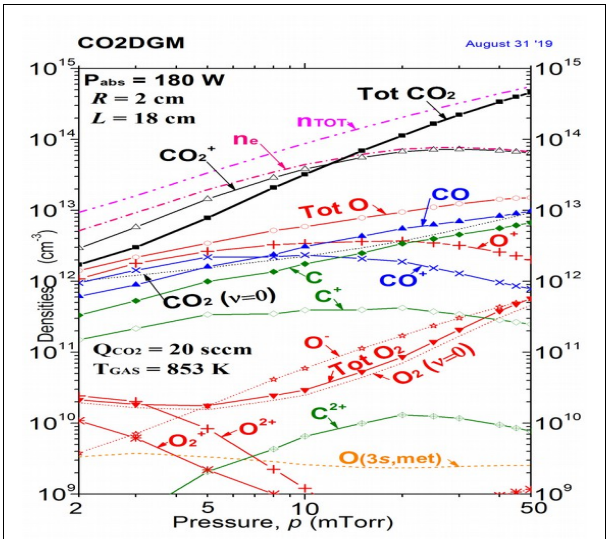

Fig. 2. Pressure depending PCC for 180 W absorbed power

CO2DGM results obtained for a three times higher P_{abs} value of 180 W are illustrated in Fig. 2. In comparison with Fig. 1, this figure shows higher ionization of the propellant with higher values of n_e and reveals a more reactive chemical situation. Ionization shown in the PCC of Fig. 2 is slightly higher for low pressures than this in Fig. 1 but becomes about four times higher for a pressure value of 50 mTorr. With 180 W of P_{abs} the CO density is nearer to the density of CO_2 than before and the CO^+ density even higher than the CO one for low pressure values. Density of O is the higher for neutral components after CO_2 but quite higher than this of CO. Consequently, the presence of O^+ is higher than the presence of CO^+. Due to the increased P_{abs} the C^+ density is about an order of magnitude higher than before and a curve giving the C^{2+} density appears for high pressures. The presence of O_2^+ and of O^{2+} is more significant than in Fig. 1, although diminishing with increasing pressure, while this of the metastable O (3*s*) species increases marginally. Finally, the electronegativity is lower than before but only for low pressure values.

Comparison of the overall features shown in the PCCs of Figs. 1 and 2 reveals a lack of any special characteristic related with the variation of the components densities coming from the increase of P_{ABS} from 60 W to 180 W. Ionization shown in the PCC of Fig. 2 is slightly higher for low pressures than this in Fig. 1 but it becomes about four times higher for a pressure value of 50 mTorr.

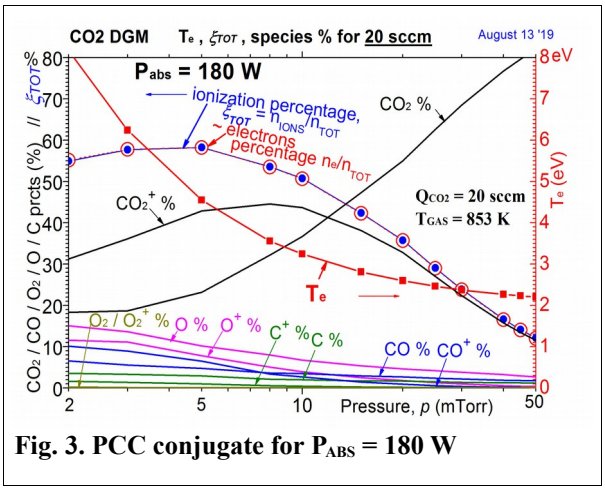

Fig. 3. PCC conjugate for P_{ABS} = 180 W

Fig. 3 presents a diagram concomitant to the PCC diagram given in Fig. 2, which provides additional information for the investigated case. Total ionization percentage $\xi_{TOT} = n_{IONS} / n_{TOT}$ is shown in this figure by blue full circles with n_e percentage also shown by bigger red empty circles. Results for ξ_{TOT} and n_e percentages coincide, which indicates that no considerable amount of doubly ionized species exists. Hence, no doubly ionized species are reported at the bottom of the figure. The sole neutral molecule with an important percentage is CO_2 with CO_2^+ keeping a similar importance for the molecular ions case. Neutral and singly ionized oxygen species percentages follow diminishing in a similar way when pressure increases. Inversely, the CO_2 presence increases with *p*, because with the available power remaining the same there is not enough dissociation, while presence of CO_2^+ diminishes because increase of pressure hampers the ionization. CO and C species and their ions follow the oxygen case.

PCC diagrams described in Figs. 1 and 2 provide snapshots of the plasma composition under various conditions for a CO_2-fueled thruster. Furthermore, similar PCC diagrams valid for higher absorbed power values have been evaluated using CO2DGM. The entirety of these PCC diagrams and of their concomitant ones like Fig. 3, can be presented together in a FD, a digest diagram giving a synoptic view of the ET functioning which we address in the following. Such a diagram is illustrated in Fig. 4. It contains the total ionization percentages of the plasma components for absorbed power values from 30 W to 2 kW as a function of the pressure. Ionization percentages are presented following iso-baric and iso-thermal curves (violet curves with stars and orange curves with circles correspondingly) and constitute a pressure depending FD describing the functioning of the related ET. It can be seen in Fig. 4 that, once the propellant feed is selected, the ionization level depends on the total pressure and on the absorbed power. Curves belonging to the higher P_{abs} values stay longer in high ionization percentage values when pressure increases, because in case of low P_{abs} values the provided power is mostly spend to chemical reactions.

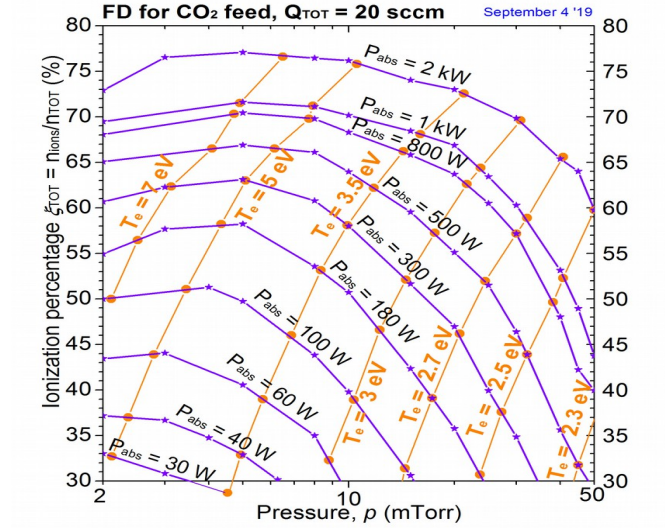

Fig. 4. Pressure dependent FD, 30 W to 2 kW absorbed power

It is to be noted that, as we address here an ISRU type technology, the availability of the propellant becomes an important issue only for missions outside the MATM, as are the Near Mars Trips (NMT). In this case the CO_2 propellant has to be collected from MATM and stored. However, in case of existence of an ample propellant amount, sufficient power must be also available in order to ionize the propellant in a satisfactory degree without spending a substantial part of the provided energy in promoting chemical reactions. In order to address the absorbed power amount in priority, it is recommended to invert the pressure dependent FD of Fig. 4 by putting the ionization and the absorbed power as coordinates. Such a form of inverted FD is presented in Fig. 5. The temperature curves in this figure bear the same orange color, with pressure curves shown in violet. It can be seen in Fig. 5 that in case of low pressure (and temperature) values the curves follow a rather diagonal direction showing a monotonous ionization increase with P_{abs}. However, for high values of P_{abs} the almost draw lines of pressures (and temperatures) show a faster increase corresponding to an easier ionization, because proportionally, a smaller amount of the spent power is devoted to chemical reactions.

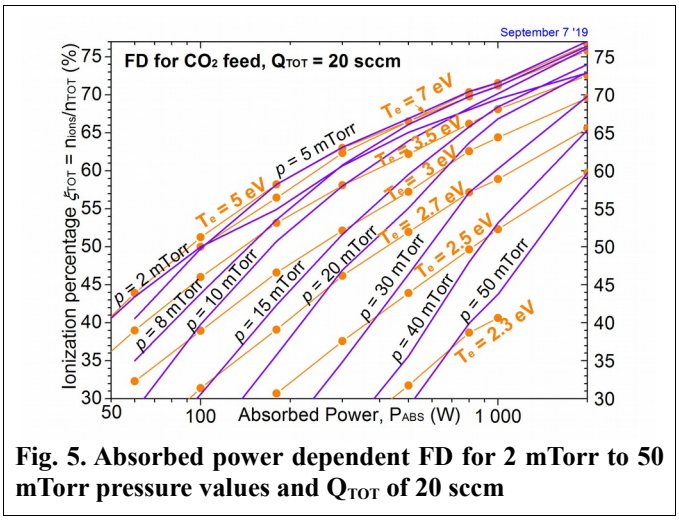

Fig. 5. Absorbed power dependent FD for 2 mTorr to 50 mTorr pressure values and Q_{TOT} of 20 sccm

3. PCC and FD diagrams addressing a higher CO_2 feed of 50 sccm

In case of ISRU based propulsion the propellant is easier to obtain, therefore results obtained with a higher CO_2 feed should be of interest. Accordingly, a feed of 50 sccm is addressed in this section. Because of the expected increased pressure of CO_2 , considered pressure values are contained in a slightly restrained domain, between 10 mTorr and 50 mTorr. The range of P_{ABS} values addressed is also somewhat increased, going from 300 W to 3 kW.

A typical PCC diagram belonging to absorption of 1 kW power by a CO_2 propellant fed in the thruster at a total flow rate of Q_{TOT} = 50 sccm is presented in Fig. 6, pertaining to a cylindrical plasma similar to the one addressed in the previous section with form factor of L = 18 cm length and R = 2 cm radius.

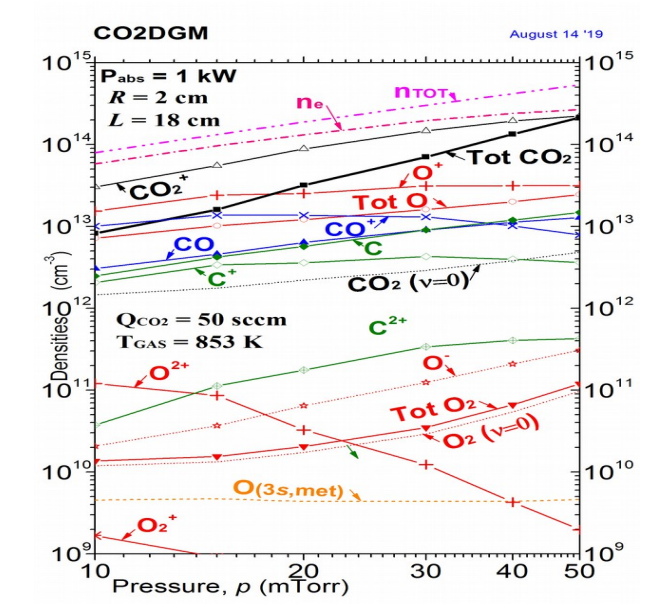

Fig. 6. Pressure depending PCC for 1 kW absorbed power

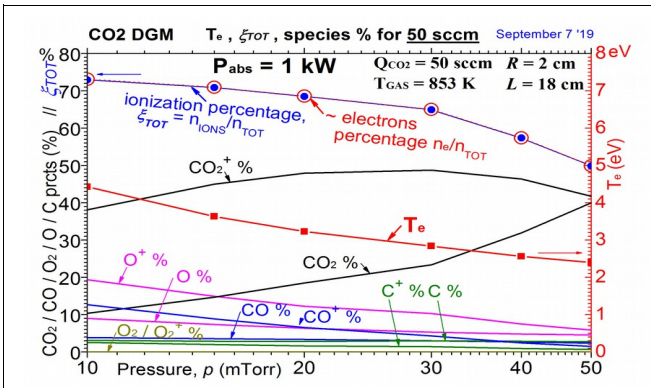

Fig. 7. PCC conjugate for P_{ABS} = 1 kW

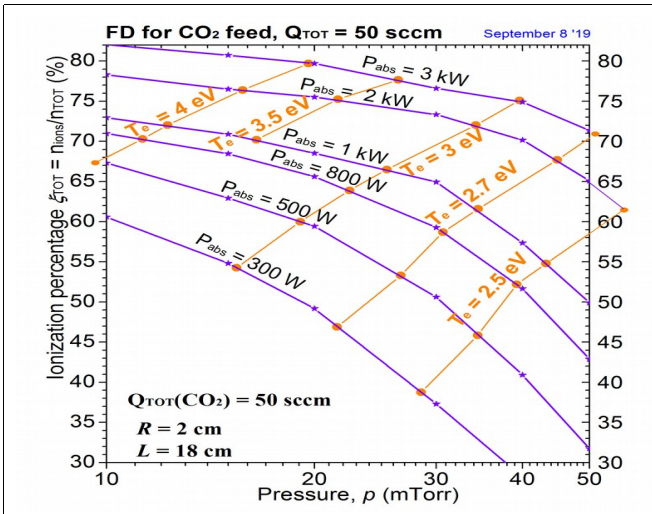

Fig. 8. Pressure dependent FD, 300 W to 3 kW absorbed power

In comparing the PCC shown in Fig. 6 with those presented in the previous section, we see that even if the feed is here of 50 sccm instead of the previously addressed 20 sccm, the P_{ABS} value of 1 kW is sufficient to ionize the CO_2 to an increased level, with the main ionized component CO_2^+ reaching a clearly higher abundance level than the CO_2 one. O^+ species are the more abundant after the CO_2^+ ones, almost an order of magnitude higher than the C^+ species. Neutral oxygen species are also more present than the carbon ones due to an increased dissociation, but no more than two or three times. However, this could contribute to show more intense oxygen than carbon lines in the visible region of their first order spectra. Doubly ionized oxygen and carbon species are quite scarce and may appear only at the bottom of the Fig. 6. Electronegativity is quite low in this case and increases with pressure while O_2 molecules are scarce.

As was the case with the propulsion oriented PCC shown in Fig. 2 of Section 2, we provide additional insight on the plasma situation by means of Fig. 7 which contains information concomitant to this of Fig. 6 presented in a similar way with Fig. 2. In Fig. 7 we observe that singly ionized species constitute the bulk of ionic species, therefore ξ_{TOT} values are again not distinguishable from the n_e ones. The sole neutral molecule with important percentage is CO_2 but, because of the high ionization, it begins with about 10 % for 10 mTorr and increases up to no more than 40 % when a 50 mTorr pressure is reached. Small presence of other molecules and of atoms is to be observed at the bottom of Fig. 7. Important presence of molecular ion is only this of CO_2^+, which has values around 40% throughout. Next ionized species is the singly ionized oxygen, with other molecular and atomic species percentages following. As expected, all ionized species show diminishing percentages when pressure increases.

Extensive numerical calculations based in CO2DGM gave a number of PCC diagrams for pressures from 10 mTorr to 50 mTorr, belonging to power absorption values between 300 W and 3 kW. Conjugate diagrams like the one shown in Fig. 7 have been also obtained. These results are presented in a condensed form in Fig. 8, which in fact constitutes a FD diagram similar to the one shown in Fig. 4 but for feeds with a higher total flow rate value of Q_{TOT} = 50 sccm. In Fig. 8, no pressure values lower than 10 mTorr are reported, because for the addressed high P_{ABS} values, even for 300 W a considerable ionization percentage of about

60 % is obtainable. It can be observed that the increase of pressure destroys the propellant ionization, but if in an ISRU context an ample amount of propellant is available this is not an important problem.

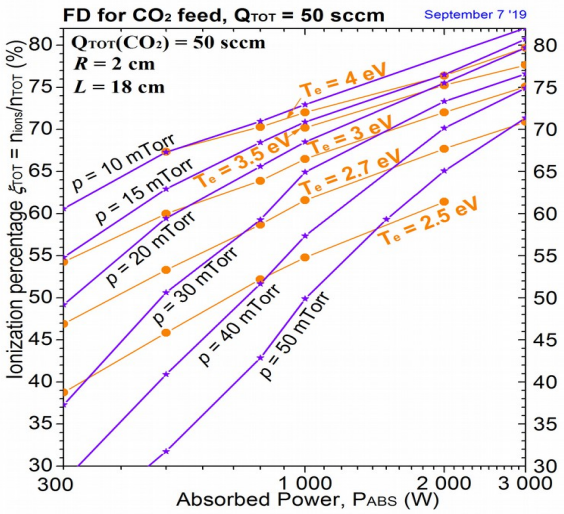

Fig. 9. Absorbed power dependent FD for 10 mTorr to 50 mTorr pressure values and Q_{TOT} of 50 sccm

Note that after exceeding an amount of absorbed power of typically P_{ABS} = 300 W, the possibility to further increase P_{ABS} is of interest essentially for thrusters functioning in rather high pressure values, where sufficient ionization percentage depends on such values.

Additional improved insight of the expected functioning of the thruster can be obtained with the help of Fig. 9, which in fact constitutes an inverted form of the FD presented in Fig. 8. Fig. 9 is analogous to Fig. 5 but for higher values of the parameters, with a Q_{TOT} value of 50 sccm and P_{ABS} varying from 300 W to 3000 W. Comparison of Figs. 5 and 9 shows a slower ionization of the propellant with lower electron temperatures due to the increase of Q_{TOT} from 20 sccm to 50 sccm.

4. PCC and FD diagrams addressing entry to a CO_2 atmosphere

As was reported previously[2], CO2DGM is also of interest to the entry in the Martian atmosphere. Note that in this case the pressure varies very fast and special attention must be payed to the variation of the pressure which may attend much higher values than the 20 mTorr or 50 mTorr addressed previously in Sections 2 and 3. The range of P_{ABS} values addressed in this section with Mars entry in mind goes from 3 kW to 25 kW, with the previously addressed significant feed value of Q_{TOT} = 50 sccm remaining the same. Similar conditions prevail in the PWK3 facility available at *IRS*, in which the provided spectra were acquired.

In comparing the obtained PCC for these conditions with the analogous ones presented in the previous sections, we have seen that, even if the feed remains at Q_{TOT} = 50 sccm, values of absorbed power as high as P_{ABS} = 20 kW are not sufficient to ionize the CO_2 to a considerable level, due to the much higher pressure values addressed. In fact, because the pressure level is of more than one Torr, ionized species remain very scarce, with the CO_2 abundance level around 90 %, clearly higher than this of the most abundant ionized component which is CO_2^+ . Presence of neutral oxygen and carbon species is quite lower than the CO_2 one. However, intense oxygen I and carbon I lines in the visible spectral region, while O and C ionic lines are not present, as we see in the next section.

5. Spectra of high pressure CO_2 plasma and applications

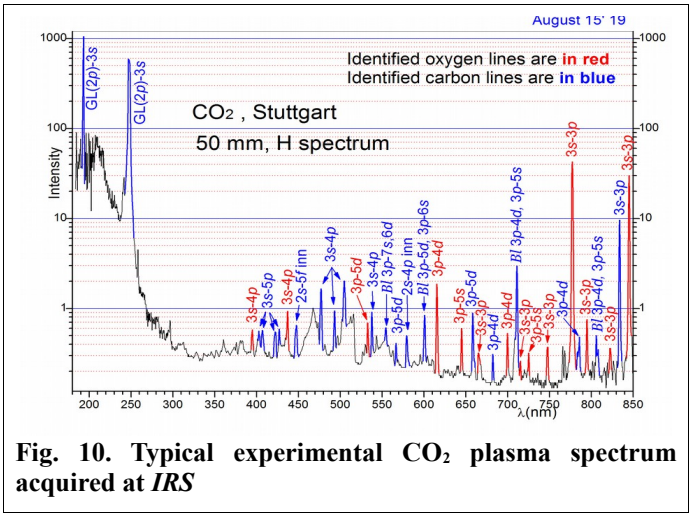

Fig. 10. Typical experimental CO_2 plasma spectrum acquired at *IRS*

Besides various methods of optical diagnostics successfully used in CO_2 plasma studies[1] we propose here a non-perturbing OES diagnostics based on the theoretical first spectra calculations obtained by CO2DGM, pertaining to both oxygen and carbon species. Note that CO spectra and also the often used for optical diagnostics[1] Swan bands pertaining to C_2 are not calculated by CO2DGM.

On the basis of the theoretical spectra we attempted a OES diagnostics of the IPG device by comparison with experimental spectra acquired[6,15] in the PWK3 device at *IRS* as a sequel of previous work[16-18]. An overview of studies of Martian like CO_2 - N_2 mixture by inductively coupled plasma torch can be found in Ref. 19 and references therein.

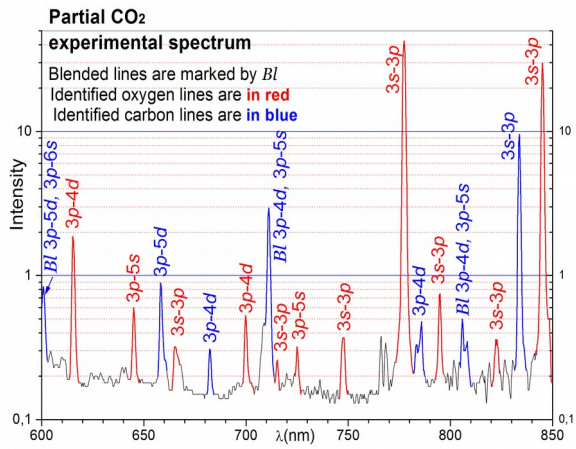

Fig. 11. Experimental C and O plasma spectrum in the 600 nm to 850 nm region

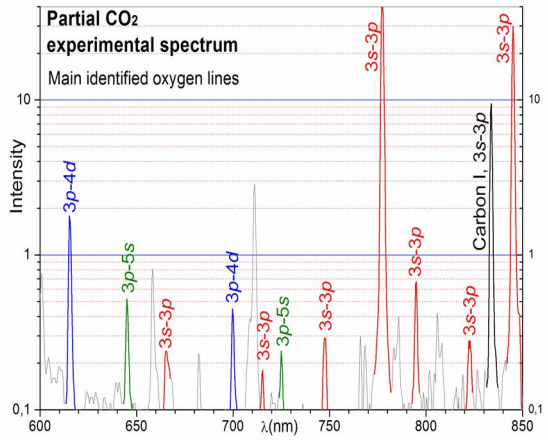

Fig. 12. Experimental O spectrum in the 600 nm to 850 nm region, including also the main C line

We present in Fig. 10 a typical experimental spectrum acquired at *IRS*, covering a large wavelength domain from 180 nm to 850 nm. We identify prominent lines of oxygen and of carbon first order spectra indicated by red and blue color correspondingly, including reference to the multiplet to which each line belongs. Lines involving an inner shell are noted by "inn" and blended lines are identified by "Bl". C_2 Swan bands are clearly visible, but no ionic oxygen or carbon lines are visible, in concordance with our low ionization results from CO2DGM. Although the resonant lines shown at the left part of Fig. 10 are much more intense than the transitory ones, they are cumbersome to handle in case of OES diagnostics because of their short wavelengths. In Figs. 11 and 12 we show spectral lines belonging to the first spectrum of oxygen and carbon, which are interesting for OES because no complete sets of 3*s* - 3*p* multiplet lines are available for both oxygen and carbon. Spectrum is contained in the 600 nm to 850 nm wavelengths region and contains pertinent lines of both the plasma constituting elements. Figs. 11 and 12 present in fact a part of Fig. 10 conveniently zoomed. Experimental spectral lines of O I acquired in the addressed region are prevailing, suggesting comparison with the theoretical ones from CO2DGM. Fig. 12, shows in colors only the O I experimental lines with the corresponding cores occasionally given in parenthesis.

The C I lines are shown in Fig. 12 with faint gray, except for a line of the leading carbon multiplet 3*s* – 3*p* which is shown in black. This most intense C I line in this region is shown for comparison with the O I spectrum. A choice of the pertinent calculated lines in the same region with intensities adapted to the experimental ones are shown in Fig. 13. It includes only lines of the first oxygen spectrum, except the intense 3*s* - 3*p* carbon line used for comparison with the C I intensity in the experimental spectrum.

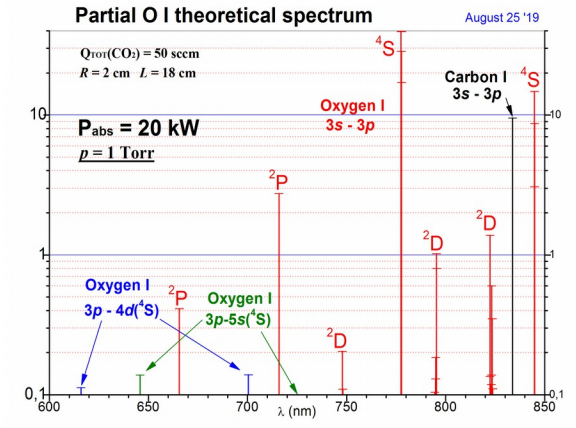

Fig. 13. Theoretical C and O plasma spectrum in the 600 nm to 850 nm region

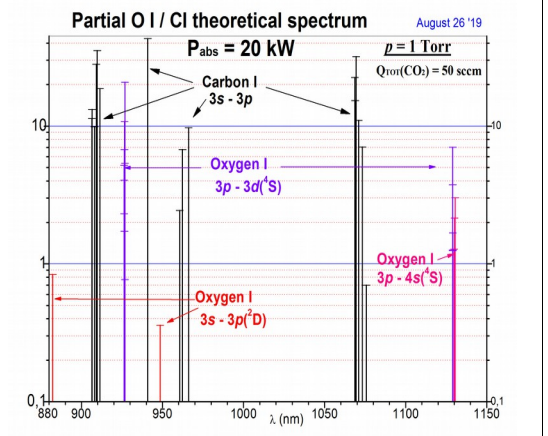

Fig. 14. Theoretical C and O plasma spectrum in the 880 nm to 1150 nm region

Line intensities in Figs. 12 and 13 have similar patterns, therefore, following our calculations, we infer that T_e values approach T_e = 2 eV and n_e is about $n_e = 10^{14}$ cm^{-3} for a CO_2 feed of Q_{TOT} = 50 sccm with corresponding pressure of about 1 Torr.

The obtained provisional evaluation should be improved by adapting the model initial conditions in detail. Also, in view of the low temperatures around 2 eV suggested by the modeling, experimental spectra in the larger than 850 nm wavelengths region, including the main C I lines and persistent O I ones, should be acquired. Our theoretical preview pertaining to this region for the same conditions have been obtained by CO2DGM and are shown in Fig. 14. Intensive lines of both O I and C I are shown in this figure. Notably, the theoretical spectrum contains the main part of the important neutral carbon multiplet $3s - 3p$ lines shown in black and persistent lines of the neutral oxygen multiplets $3s - 3p$ in red, $3p - 3d$ in purple, and $3p - 4s$ in pink.

6. Conclusions and perspectives

We conclude that PCC and FD diagrams and theoretical oxygen and carbon spectra from CO2DGM contribute efficiently to theoretical characterization and to diagnostics of low power CO_2-fueled ETs. In order to obtain an interesting comparison, higher power class thrusters have been also successfully addressed. The case of very high values of absorbed power was also approached, mainly because of its interest for entry in atmospheres with CO_2 as main component. Notably, an example of OES application pertaining to the latter case is illustrated, justifying the manifested very low plasma ionization under high pressure values: Ionic spectral lines are practically absent in this case.

Although molecular CO_2 spectra are also present in the plasma, addressed OES diagnostics was based only in the visible part of the atomic oxygen and carbon species emission, in view of the absence of ionic lines. The important comparison of the carbon / oxygen line intensities was made possible only after incorporating in the CO2DGM code a full calculation of the carbon spectrum too.

Acquisition of more experimental results will allow in general to refine characterization, optimization and diagnostics of ETs pertaining to various technologies and necessary for NMT[20]. Also, in order to obtain a more detailed diagnostics for atmospheric entry plasma, additional spectral acquisitions in the few Torr pressure domain concerning the red spectral region could be useful.

References

[1]Katsonis, K., and Berenguer, Ch., "Characterization of Low Pressure CO_2 Plasma in Space," *ESA 6th RHTG Workshop*, St Andrews, UK, November 2014

[2]Berenguer, Ch., and Katsonis, K., "Global Modeling of CO_2 Discharges with Aerospace Applications," *Advances in Aerospace Engineering*, vol. **2014**, Article ID 847097, 2014

[3]Katsonis, K., Berenguer, Ch., Gonzalez del Amo, J., and Stavrinidis, C., "CO_2 / N_2 Breathing Electric Thrusters for LMOs," *5th Space Propulsion Conference*, Paper ID SP2016_**3124972**, Rome, Italy, May 2016

[4]Berenguer, Ch., and Katsonis, K., "A Detailed Global Model for Characterization of CO_2 Fed Electric Thrusters," *Imperial Journal of Interdisciplinary Research*, **2**, 1708, 2016

[5]Mangold, N., Baratoux, D., Witasse, O., Encrenaz, T., and Sotin, C., "Mars: a Small Terrestrial Planet," *Astron. Astrophys. Rev.* 24:15, December 2016

[6]Löhle, S., Lein, S., Eichhorn, Ch., Herdrich, G., and Winter, M., "Spectroscopic Investigation of an Inductively Heated CO_2 Plasma for Mars entry simulation," *Journal of Technical Physics*, Quarterly **L**, 233, 2009

[7]Katsonis, K., and Berenguer, Ch., "CO2DGM: a Detailed Global Model for Characterization and Optical Diagnostics of CO2 Fed Electric thrusters," *Electric Propulsion Innovation and Competitiveness (EPIC) Workshop*, London, UK, 2018

[8]Katsonis, K., Berenguer Ch. and Gonzalez del Amo, J. Characterization of Air Breathing Plasma Thrusters Fueled by Atmospheric Mixtures Encountered in Earth Atmosphere at an Altitude of About 200 km, 34th IEPC Conference, IEPC-2015-**268**, Kobe, Japan, 2015

[9]Katsonis, K., Berenguer, Ch., Gonzalez del Amo, J., and Stavrinidis, C., "Diagnostics of Air-Breathing Electric Thrusters by Optical Emission Spectroscopy," *5th Space Propulsion Conference*, Paper ID SP2016_**3124973**, Rome, Italy, May 2016

[10]Katsonis, K., and Berenguer, Ch., "Characterization and diagnostics of CO_2 fed electric thrusters by using CO2DGM model of DGM type," update of *ResearchGate project : ISRU Based Electric Propulsion*, June 2018

[11]Katsonis, K., Berenguer, Ch., "Characterization and Optical Diagnostics of CO_2 Fed Electric Thrusters by Using a Detailed Global Model," *6th Space Propulsion Conference*, Paper ID SP2018_**237**, Seville, Spain, May 2018

[12]Katsonis, K., Berenguer, Ch., "Characterization and Optical Diagnostics of CO_2 Fed Electric Thrusters by Using a DGM," *6th Space Propulsion Conference*, Poster, Seville, Spain, May 2018

[13]Berenguer, Ch., and Katsonis, K., "Detailed Global Modeling in Support of Electric Propulsion and Throttling of Common Propellants," *6th Space Propulsion Conference*, Paper ID SP2018_**245**, Seville, Spain, May 2018

[14]Katsonis, K., and Berenguer, Ch., "Study of CO_2 Plasmas of Interest to Space Applications Based on a Detailed Global Model," *7th ESA RHTG Workshop*, Stuttgart, Germany, November 2016

[15]Herdrich, G., Marynowski, T., Dropmann M., and Fasoulas, S., "Mars and Venus Simulation Capabilities of IRS Plasma Wind Tunnel PWK3," *Applied Physics Research*, Vol. **4**, No. 1, pp. 146-155, February 2012

[16]Herdrich, G., Auweter-Kurtz, M., Kurtz, H. L., Laux, T., and Winter, M., "Operational Behaviour of the Inductively Heated Plasma Source IPG3 for Re-entry Simulations," *Journal of Thermophysics and Heat Transfer*, Vol. **16**, No. 3, pp. 440-449, July--September 2002

[17]Herdrich, G., Auweter-Kurtz, M., Endlich, P., and Kurtz, H., "Mars Entry Simulation using the Inductively Heated Plasma Generator," *Engineering Note, Journal of Spacecrafts and Rockets*, Vol. **40**, No. 5, pp. 690-694, Sept.-Oct. 2003

[18]Winter, M., Herdrich, G., Lein, S., Steinbeck, A., Eichhorn, C., and Fertig, M., "Results of CO_2 Plasma Diagnostic Measurements using PWK3," Universität Stuttgart presentation, October **2007**, Institut für RaumfahrtSysteme, www.irs.uni-stuttgart.de

[19]Vacher, D., André, P., and Dudeck, M., "Overview on Studies of Martian Like CO_2 - N_2 Mixture by Inductively Coupled Plasma Torch," *3rd ESA RHTG Workshop*, Heraklion, Greece, September 2008

[20]Katsonis, K., and Berenguer, Ch., "CO_2 based ISRU propulsion for satellites and spacecrafts near Mars / ISRU-MARS," update of *ResearchGate project : CO2 based ISRU propulsion for satellites and spacecrafts near Mars / ISRU-MARS*, July 2019